

Global Reconstruction of Neuronal Fibres

Marco Reisert¹, Irina Mader^{2,3}, and Valerij Kiselev¹

¹ Dept. of Diagnostic Radiology, Medical Physics, University Hospital Freiburg

² Section of Neuroradiology, Neurocentre of University Hospital Freiburg

³ Freiburg Brain Imaging Centre, Department of Neurology, University Hospital Freiburg

reisert@informatik.uni-freiburg.de

Abstract. Fibre tracking algorithms follow two paradigms: Local tracking approaches are based on the 'walker' principle, the fibres are reconstructed path-by-path by small successive steps along the tracts. On the other hand global ideas try to reconstruct all fibres at once by optimizing a certain global objective. Local algorithms are fast but suffer from accumulated errors. Global methods have a more sound foundation but are very complex to optimize. This paper presents a novel approach which fuses both ideas while keeping their advantages. The core is a Bayesian approach which formulates the tracking result as a maximum a posteriori estimate. The optimization is based on a spatial point process optimized with a Metropolis-Hastings sampler. The key idea is to use local methods within the optimization process to approach the global optimum efficiently. The experiments show that the approach is nearly two orders of magnitude faster than recent global approaches while keeping the detection performance.

1 Introduction

Fibre tracking is a method for the reconstruction of neuronal pathways using measurements of the anisotropic diffusion of water molecules in the fibrous structure of white matter [1–4]. Such information is made available by a recent advance in magnetic resonance imaging (MRI). Fibre tracking promises a high impact in fundamental neuroscience and its clinical applications.

The approaches can be divided into two groups: local and global methods. Local methods construct fibres independently path-by-path, the fibres do not influence each other. The reconstruction of long neuronal pathways is performed in small successive steps, either deterministic [3, 4] or probabilistic [5, 6] by following the local, voxelwise defined distribution of fibre directions. The advantage of local methods is that they are rather fast, but they also have several problems. The most apparent is probably that a minor imperfection in the rule of performing local steps can accumulate and significantly affect the final result. On the other hand, global methods try to reconstruct the fibres all at once. This gives the reconstruction a larger field of view when an ambiguous area has to be resolved. Each curve is assigned a probability measure that takes into account both the likelihood with the measured diffusion-weighted signal and *a priori* anatomical

knowledge. The early methods [7] had several limitations that did not allow to reveal the full potential of the approach. A recently developed implementation of the global approach called the "Gibbs-tracking" [8] is free from these drawbacks. It works with High-Angular-Resolution-Diffusion data (HARDI) with arbitrary number of diffusion weighting directions. In the reconstruction algorithm, the curves representing the neuronal fibres are built from small fibre segments with continuously varying positions, orientations and density. But the problem with such kind of methods is the high computational expense (in [8] one month on a common Desktop PC for the whole brain) and bad scalability. In this paper we propose a novel fibre reconstruction method that fuses local and global ideas. The approach is global, and thus, shares all the advantages while it uses local methods to approach the global optimum which makes the algorithm practical useable. Our idea builds on approach by Kreher et al [8]. Similar ideas are also used to extract road networks from aerial images [9]. The reconstruction problem is formulated as an energy minimization problem on a spatial point process [10] using the Metropolis-Hastings algorithm for optimization. The major difference of our approach to [9,8] is the extension of the usual 'soup of segment' representation to a graph-like model where the connection between segments are modeled explicitly.

The paper is organized as follows: In the next section we present the fibre model and the associated energies. In Section 3 the optimization algorithm is presented with all details. In the last Section we discuss the differences of our approach to recent algorithms and give some preliminary results with an in vivo dataset showing that the proposed approach is able to make a global reconstruction (with about 10^5 fibres) of the whole brain in reasonable time (below one day on a standard PC) while detecting even difficult fibre bundles.

2 Global Fibre Tracking

We denote an abstract model of the global fibre configuration by \mathcal{M} and the measured HARDI-signal by $D = S/S_0$. We want to maximize the a-posteriori probability $P(\mathcal{M} | D)$ with respect to \mathcal{M} , i.e. we want to find the most likely model given the observed data. We follow Bayes' theorem and assume the usual exponential model for the prior $P(\mathcal{M})$ and data-likelihood $P(D | \mathcal{M})$.

$$P(\mathcal{M} | D) = \frac{1}{Z} \exp(-E_{\text{int}}(\mathcal{M}) - E_{\text{ext}}(\mathcal{M}, D)),$$

where Z is the partition function. The design of the external energy has to express the dissimilarity between the data and the hypothetical model. In order to find such a measure, it is natural to use a simple model of the physical imaging process mapping a given fibre configuration \mathcal{M} onto a hypothetical measurement $F_{\mathcal{M}}$ and compare this outcome with the actual measurement D . The internal energy should drive the fibres to be like fibres observed in nature in terms of smoothness, regularity and length. In the following we explain how the model \mathcal{M} is described and how the internal and external energy is formulated.

2.1 The Discrete Model

A fiber segment (particle) is described by a spatial position $\mathbf{x} \in \mathbb{R}^3$ and an orientation $\mathbf{n} \in S_2$. The segment is the basic building block of the fibre model. Formally we refer to a fibre segment by the tuple $X = (\mathbf{x}, \mathbf{n})$. Picture the fibre segment as a small thin tube of length 2ℓ , i.e. the endpoints of the tube are at position $\mathbf{x} + \ell\mathbf{n}$ and $\mathbf{x} - \ell\mathbf{n}$, respectively. Below we have to refer to one of the endpoints explicitly, we write X^+ for the endpoint associated with $+\mathbf{n}$ and for the opposite endpoint associated with $-\mathbf{n}$ we write X^- . An ensemble of segments is denoted by $\mathcal{X} = \{X\}$ and we denote the number of segments by N . Besides the ensemble of segments \mathcal{X} there is a set of connections or edges, denoted by $\mathcal{E} = \{E\}$. An edge $E \in \mathcal{E}$ connects the endpoints of two distinct segments. Mathematically, we deal with an edge-attributed graph, i.e. an edge E connects two segments while it carries the additional information via which of the endpoints this is done. Formally, we express this by using the above notation and write $E = (X_1^{\alpha_1}, X_2^{\alpha_2})$ where $X_i \in \mathcal{X}$ and $\alpha_i \in \{+, -\}$. In this way we can easily enforce restrictions like the absence of Y-junctions and cycles.

2.2 Internal Energy

Based on the above definitions we write the internal energy as follows

$$E_{\text{int}}(\mathcal{M}) = \lambda_{\text{int}} \sum_{(X_1^\alpha, X_2^\alpha) \in \mathcal{E}} U_{\text{con}}(X_1^{\alpha_1}, X_2^{\alpha_2}).$$

where $U_{\text{con}}(X_1^{\alpha_1}, X_2^{\alpha_2})$ refers to the interaction potential between two connected segments $X_1 = (\mathbf{x}_1, \mathbf{n}_1)$ and $X_2 = (\mathbf{x}_2, \mathbf{n}_2)$. The parameter $\lambda_{\text{int}} \in \mathbb{R}^+$ is just a fixed parameter determining the 'strength' of the energy. Note that only connected fiber segments contribute to the internal energy. The potential U_{con} should basically fulfill three requirements: first, the effect should be a kind of attracting force, such that two connected endpoints stay together while they are connected. And secondly, the resulting fiber, i.e. the consecutive coordinates $\mathbf{x}_1, \mathbf{x}_2$ should be consistent with the internal orientations \mathbf{n}_1 and \mathbf{n}_2 , more precisely the connecting line $\mathbf{x}_1 - \mathbf{x}_2$ should have approximately the same direction as \mathbf{n}_1 and \mathbf{n}_2 . This includes that the curvature of the fiber should be kept small, meaning that \mathbf{n}_1 and \mathbf{n}_2 should not differ too much. We found a quite simple energy fulfilling the above requirements in an implicit manner. To formulate this potential we use the abbreviation $\bar{\mathbf{x}} = \frac{\mathbf{x}_1 + \mathbf{x}_2}{2}$ for the midpoint of line connecting the two segments.

$$U_{\text{con}}(X_1^{\alpha_1}, X_2^{\alpha_2}) = \frac{1}{\ell^2} (\|\mathbf{x}_1 + \alpha_1 \ell \mathbf{n}_1 - \bar{\mathbf{x}}\|^2 + \|\mathbf{x}_2 + \alpha_2 \ell \mathbf{n}_2 - \bar{\mathbf{x}}\|^2) - L$$

Basically, the potential is composed of the squared distances from the endpoints of the segments to the midpoint of the line connecting both. For an illustration see Figure 1. The two parameters that occur are the length $\ell > 0$ (actually half the length) of the fiber segment and a bias L . The bias L is a kind of connection

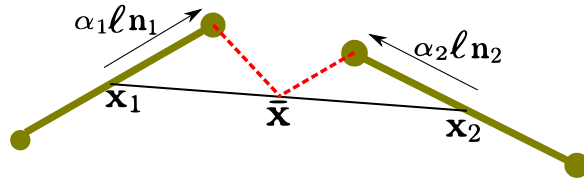


Fig. 1. The internal energy between two segments. The segments are given by their midpoints $\mathbf{x}_1, \mathbf{x}_2$ and their orientations $\mathbf{n}_1, \mathbf{n}_2$. The red dotted lines indicate the distances which are minimized.

likeliness (physicists would say it is the chemical potential of a connection). Large $L > 0$ imply a high likeliness that two segments link together. The first two terms drive the segments to be close together (but not closer than the length of the segments) and secondly it forces the connecting line to be along the internal fiber directions \mathbf{n}_1 and \mathbf{n}_2 . Another advantage of this energy is that it is quadratic in its constituents. Thus, we can solve it analytically for optimal configurations. Two situations can arise. Only one endpoint of a particle is connected or both. First consider the simple one, without restriction of generality the negative endpoint of particle X_2 is connected with another endpoint X_1^+ . That is, the internal energy is just $U(X_1^+, X_2^-)$. Assume now X_2 can move freely while X_1 is fixed. The optimal configuration for X_2 can be easily guessed:

$$\mathbf{x}_2 = \mathbf{x}_1 + 2\ell\mathbf{n}_1 \text{ and } \mathbf{n}_2 = \mathbf{n}_1, \quad (1)$$

that is, X_2 has the same orientations as X_1 and is seamless connected to X_1 . The second situation is a little bit more difficult. Consider now three elements X_1, X_2, X_3 connected subsequently such that the connection energy is $U_{\text{con}}(X_1^+, X_2^-) + U_{\text{con}}(X_2^+, X_3^+)$. Now, we can ask again, what is the energy minimizing configuration of X_2 while X_1, X_3 are fixed. With basic algebra one finds that

$$\mathbf{x}_2 = \frac{\mathbf{x}_1 + \ell\mathbf{n}_1 + \mathbf{x}_3 + \ell\mathbf{n}_3}{2} \text{ and } \mathbf{n}_2 = \frac{\mathbf{x}_3 - \mathbf{x}_1}{\|\mathbf{x}_3 - \mathbf{x}_1\|}. \quad (2)$$

Later, we need both results for a proposal in the Metropolis-Hastings algorithm.

2.3 External Energy

The external energy is based on the squared difference between the measured signal D and a predicted signal based on the fibre model \mathcal{M} . We denote this predicted signal by $F_{\mathcal{M}} : \mathbb{R}^3 \times S_2 \mapsto \mathbb{R}$, it is a scalar function defined on the Position-Orientation-Space (POS), where the position refers to the spatial position and the orientation to the fibers's direction. The predicted signal is of the same type as the measured signal $D : \mathbb{R}^3 \times S_2 \mapsto \mathbb{R}$. We will interpret both as continuous fields despite the fact the data is represented on a discrete grid. Concerns coming from the discrete nature of the data will be discussed later.

Now, how to create the 'HARDI'-signal from the high-level fibre representation \mathcal{M} ? In position space we let a segment contribute to the field by an isotropic Gaussian blob of width $\sigma \in \mathbb{R}^+$. In orientation space we adopt the usual single diffusion tensor model. Given fibre model \mathcal{M} the predicted signal takes the form

$$F_{\mathcal{M}}(\mathbf{x}, \mathbf{n}) = w \sum_{i=1}^N e^{-c(\mathbf{n}^T \mathbf{n}_i)^2} e^{-|\mathbf{x} - \mathbf{x}_i|^2 / \sigma^2},$$

where each segments contributes to the field with the same weight $w \in \mathbb{R}^+$. The parameter $c \in \mathbb{R}^+$ is the width of the fibre in orientation space. The external energy itself is just the squared L_2 -norm (on the POS space) of the measured data D and the signal generated by \mathcal{M} , i.e.

$$E_{\text{ext}}(\mathcal{M}, D) = \lambda_{\text{ext}} \|F_{\mathcal{M}} - D\|^2 = \lambda_{\text{ext}} \int_{\mathbb{R}^3 \times S_2} |F_{\mathcal{M}}(\mathbf{x}, \mathbf{n}) - D(\mathbf{x}, \mathbf{n})|^2 d^3\mathbf{x} d^2\mathbf{n},$$

where λ_{ext} is the 'strength' of the external energy. Thinking about the implementation issues it is, of course, much too expensive to compute this difference by first generating the hypothetical signal and then computing the norm. Secondly, we have to keep in mind that for energy minimization only energy differences come into account, absolute values are not significant. Thus, we write out the energy $E_{\text{ext}}(\mathcal{M}, D) = \|F_{\mathcal{M}}\|^2 - 2\langle F_{\mathcal{M}}, D \rangle + \|D\|^2$ and consider the first and second term more detailed. The third term is an overall constant and can be omitted. Actually, the first term does not depend on the data field D . To get a representation for $\|F_{\mathcal{M}}\|^2$ which suites better for an efficient implementation we integrate pair by pair and get

$$\|F_{\mathcal{M}}\|^2 = Cw^2 \sum_{i=1}^N \sum_{j=1}^N I_0(c|\mathbf{n}_i^T \mathbf{n}_j|) e^{-\frac{|\mathbf{x}_i - \mathbf{x}_j|^2}{2\sigma^2}}$$

where $I_0(c|\mathbf{n}_i^T \mathbf{n}_j|)$ denotes the integral $\int_{S_2} e^{-c(\mathbf{n}^T \mathbf{n}_i)^2} e^{-c(\mathbf{n}^T \mathbf{n}_j)^2} d\mathbf{n}$ which can be precomputed for efficient evaluation of energy differences. For segment X_i only segments in a small range $\|\mathbf{x}_i - \mathbf{x}_j\| \sim \sigma$ fall into account. Now, consider the second term which depends on the data. Just by inserting the model we get

$$\langle F_{\mathcal{M}}, D \rangle = \sum_{i=1}^N w \int_{\mathbb{R}^3 \times S_2} e^{-c(\mathbf{n}^T \mathbf{n}_i)^2} e^{-\frac{|\mathbf{x}_i - \mathbf{x}|^2}{\sigma^2}} D(\mathbf{x}, \mathbf{n}) d^3\mathbf{x} d^2\mathbf{n} = Cw \sum_{i=1}^N D^{\text{eff}}(\mathbf{x}_i, \mathbf{n}_i),$$

thereby D^{eff} is the HARDI-signal convolved with the kernel $e^{-c(\mathbf{n}^T \mathbf{n}')^2} e^{-|\mathbf{x} - \mathbf{x}'|^2 / \sigma^2}$. In fact, for small σ and large c the D^{eff} is the Funk Radon-transform (FRT) of the HARDI-signal. And this is what we actually do in practice, we use the FRT for D^{eff} which keeps the angular dependency more selective. To evaluate the discrete represented D^{eff} at continuous coordinates (\mathbf{x}, \mathbf{n}) we just use linear interpolation in all 5 'directions' in POS. For the 2 angular coordinates we use a kind of barycentric interpolation, that is, for a given \mathbf{n} we search for the three

nearest data points on the sphere and compute the barycentric coordinates of these points. These coordinates are then used as interpolation weights to combine the three values originating from these three points additively. Thus, combined with the spatial interpolation we use a 5-linear interpolation. Overall, for one evaluation we combine additively $3 * 8 = 24$ values at different voxels.

3 The Metropolis-Hastings Sampler

The Metropolis-Hastings sampler is a general approach to sample high dimensional distributions whose partition function is unknown (in our case the posterior $P(\mathcal{M} | D)$). The algorithm can be used to minimize/maximize certain objectives by introducing a temperature T which controls the sharpness of the considered distribution. If the distribution is very sharp (the temperature very low) it is very likely that the optimum (or one of the extrema) is sampled. The idea is as follows: Choose a modification of the current state \mathcal{M} according to a proposal distribution p^{prop} , we call this modification \mathcal{M}' . Then, we accept this modification if the so called Green's ratio R is above 1, where R is given by

$$R = \left(\frac{P(\mathcal{M}' | D)}{P(\mathcal{M} | D)} \right)^{1/T} \frac{p^{\text{prop}}(\mathcal{M} | \mathcal{M}')}{p^{\text{prop}}(\mathcal{M}' | \mathcal{M})}.$$

If R is below 1 the modification is accepted with probability R . After a certain number of iterations (the 'burn-in' phase) the resulting chain of states follows the desired distribution. For further details and applications to particle systems as applied here see [10].

In our approach the proposal splits into three different types, where each of the proposal is selected with a certain probability: segment creation/deletion ($p_{\text{birth}}, p_{\text{death}}$), segment moves ($p_{\text{shift}}, p_{\text{opt}}$) and connecting segments (p_{fibre}). As already depicted in the beginning the last proposal is based on a tracking algorithm which is usually a 'standalone' algorithm to extract fibre tracts.

3.1 Creation/Deletion

The birth and death proposals are typical for MH-samplers and do not need to be explained in much detail. We just have to mention that in our experiments we restricted the 'playground' of our particles to the white-matter area. Thus, 'draw uniformly' in the birth proposal means that we choose uniformly a continuous coordinate \mathbf{x} inside the white matter and isotropically a direction $\mathbf{n} \in S_2$. In the following, we write $\mathcal{M}' = \mathcal{M} + X$ for the fibre configuration \mathcal{M}' which results from adding a segment X to another configuration \mathcal{M} . For deleting a particle we use the minus sign, respectively.

– **Birth Proposal** with p_{birth}

Draw a X uniformly and add to configuration \mathcal{M} with ratio

$$R = \frac{e^{-E(\mathcal{M}+X)/T}}{e^{-E(\mathcal{M})/T}} \frac{\lambda}{N+1} \frac{p_{\text{death}}}{p_{\text{birth}}}$$

Here, $\lambda > 0$ denotes the density parameter of the underlying free Poisson process.

– **Death Proposal** with p_{death}

Draw uniformly a $X \in \mathcal{X}$ and delete from configuration with ratio

$$R = \frac{e^{-E(\mathcal{M}-X)/T} N p_{\text{birth}}}{e^{-E(\mathcal{M})/T} \lambda p_{\text{death}}}$$

Both proposals depend on λ which is parameter of the underlying Poisson distribution. The meaning of λ is the expected number of segments in the considered volume. For high temperatures λ has influence on the results, but for low temperature which we are aiming at, λ is less and less important.

3.2 Particle Moves

In fact, moving a particle can be replaced by a death followed by a birth of a particle. Thus, the introduction of a random move is just for performance reasons. But we also introduced a second proposal which chooses for connected segments the optimal configuration with respect to the internal energy. We observed that this speeds up the convergence towards smooth, low-curvature fibres drastically.

– **Random Shift Proposal** with p_{shift}

Take uniformly a $(\mathbf{x}, \mathbf{n}) = X \in \mathcal{X}$ and draw a new position \mathbf{x}' and orientation \mathbf{n}' according to a proposal distribution $p_{\mathbf{x}, \mathbf{n}}^{\text{prop}}$. Call \mathcal{M}' the modified ensemble containing the moved particle. Then, accept the proposal with

$$R = \frac{e^{-E(\mathcal{M}')/T} p_{\mathbf{x}', \mathbf{n}'}^{\text{prop}}(\mathbf{x}, \mathbf{n})}{e^{-E(\mathcal{M})/T} p_{\mathbf{x}, \mathbf{n}}^{\text{prop}}(\mathbf{x}', \mathbf{n}')}$$

– **Optimal Shift Proposal** with p_{opt}

Take uniformly a $(\mathbf{x}, \mathbf{n}) = X \in \mathcal{X}$. If one endpoint of X is free and the other is connected we use equation (1) to find a new configuration $X' = (\mathbf{x}', \mathbf{n}')$. If X is connected with both endpoints to some other particles, then choose the new position \mathbf{x}' and orientation \mathbf{n}' according to equation (2). Accept the new configuration with ratio

$$R = \frac{e^{-E(\mathcal{M}')/T} p_{\text{shift}} p_{\mathbf{x}', \mathbf{n}'}^{\text{prop}}(\mathbf{x}, \mathbf{n})}{e^{-E(\mathcal{M})/T} p_{\text{shift}} p_{\mathbf{x}, \mathbf{n}}^{\text{prop}}(\mathbf{x}', \mathbf{n}') + p_{\text{opt}}}$$

For the proposal distribution $p_{\mathbf{x}', \mathbf{n}'}^{\text{prop}}(\mathbf{x}, \mathbf{n})$ we used a Gaussian-like distribution. One adds independently Gaussian meanless noise of width σ_{prop} to the endpoints $\mathbf{x}' \pm \ell \mathbf{n}'$ of the current segment and backprojects onto a length 2ℓ .

3.3 Create Connections / Fibre Tracking

As already depicted the proposal for connections $E \in \mathcal{E}$ between particles is based on a kind of tracking algorithm known from ordinary fibre tracking. The

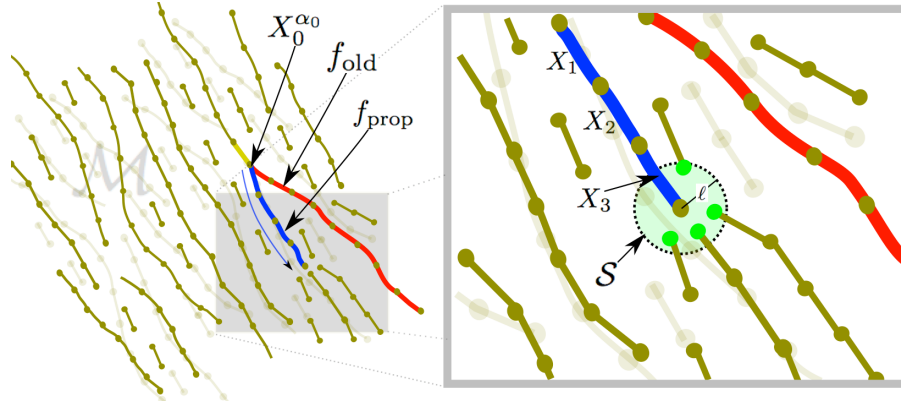


Fig. 2. The Fibre Proposal: a segment is selected (X_0^α) and the algorithm suggests to replace the pending fibre (in red) with a new track (in blue) which is generated by a simple incremental tracking algorithm. During the tracking the current segments searches for successors in a small ball around its current endpoint. The green endpoints belong to the successor set \mathcal{S} . Only free endpoints are selected as successors.

proposal does not propose just one connection E but a whole set of connection forming the part of a putative fibre. By a fibre part we think of a sequence of connections $f = (E_1, E_2, \dots)$ which connect fibre segments X_k subsequently, i.e. $f = ((X_0^\alpha, X_1^{\alpha_1}), (X_1^{-\alpha_1}, X_2^{\alpha_2}), \dots)$. We say a fibre part f is pending at X^α if f is the longest fibre part starting at X^α . In these terms the actual proposal takes the form:

– **Fibre Proposal** with p_{fibre}

Take uniformly a $(\mathbf{x}, \mathbf{n}) = X_0 \in \mathcal{X}$ and a direction $\alpha = \{-, +\}$. Denote the fibre pending at X_0^α by f_{old} and let \mathcal{M}_0 the fibre configuration without fibre f_{old} . Sample a new fibre f_{prop} according to some proposal distribution $p_{\mathcal{M}_0}^{\text{fibre}}$ and denote the resulting fibre configuration by \mathcal{M}' . Replace the old fibre by the new fibre with ratio

$$R = \frac{e^{-E(\mathcal{M}')/T} p_{\mathcal{M}_0}^{\text{fibre}}(f_{\text{old}})}{e^{-E(\mathcal{M})/T} p_{\mathcal{M}_0}^{\text{fibre}}(f_{\text{prop}})}$$

In Figure 2 a simple fibre proposal is depicted. In fact, a proposal can also close a gap between two distant parts of a putative fibre. The tricky part of this proposal is the fibre tracking itself which is above simply called 'sample a new fibre'. We adopt here techniques known from probabilistic tracking. The difference is that the actual tracking takes place on already existing segments and is, thus, only indirectly driven by the data. So the tracking is rather a hopping on the fibre segments. Suppose we start with a segment X_0^α . Now we search for successive endpoints in \mathcal{X} . In our approach we restricted the search on a ball with center $\mathbf{x}_0 + \alpha \ell \mathbf{n}_0$ and radius ℓ (as depicted in Figure 2). Call the set

of free endpoints that lie within this ball \mathcal{S} . It is known that the MH-sampler works better if the proposal distribution is roughly the same as the desired distribution. So, we will sample the new successor from \mathcal{S} with a probability $p_1^{\text{suc}}(S) = \frac{1}{Z} \exp(-U_{\text{con}}(X_0^\alpha, S)/T_{\text{prop}})$. If the successor set \mathcal{S} is empty we stop the tracking. Actually, we also have to include a 'no successor' proposal. This is necessary to keep the whole proposal reversible. For the 'no successor' proposal we assume a probability $p_1^{\text{suc}}(\emptyset) = \frac{1}{Z} e^{-0} = 1/Z$. So, the normalizing constant is $Z = 1 + \sum_{S \in \mathcal{S}} \exp(-U_{\text{con}}(X_0^\alpha, S)/T_{\text{prop}})$. If the successor $X_1^{\alpha_1} := S$ was chosen the whole procedure is repeated: new successor candidates for the opposite endpoint $X_1^{-\alpha_1}$ are selected, probabilities are computed and a successor is drawn or tracking is stopped. For the proposed fibre f_{prop} and also for the current fibre f_{old} one has to compute the proposal probability $p_{\mathcal{M}}^{\text{fbre}}(f)$. This is necessary to compute the Green's ratio. Suppose a given fibre $f = ((X_0^{\alpha_0}, X_1^{\alpha_1}), (X_1^{-\alpha_1}, X_2^{\alpha_2}), \dots)$, then the probability of proposing fiber f is just the product of all successor distributions along the fiber, i.e.

$$p_{\mathcal{M}}^{\text{fbre}}(f) = \prod_{k=0}^{n-1} p_k^{\text{suc}}(X_k^{\alpha_k})$$

The energy difference in Green's ratio is simple to compute. Since the connections do not affect the external energy we have that

$$E(\mathcal{M}') - E(\mathcal{M}) = \sum_{k \sim f_{\text{prop}}} U(X_k^{\alpha_k}, X_{k+1}^{\alpha_{k+1}}) - \sum_{j \sim f_{\text{old}}} U(X_j^{\alpha_j}, X_{j+1}^{\alpha_{j+1}}).$$

The first sum runs over the segments belonging to the proposed fibre, the second over the current fibre. From an algorithmic viewpoint we just have to accumulate the connection energies during the tracking of f_{prop} and f_{old} .

4 Discussion and Results

The big difference of our approach to Kreher's [8] is the formulation of the internal energy. Kreher modelled the connectivity implicitly by attraction forces. The attraction forces lead to unreasonable configurations like Y-junctions and double connections. Kreher avoided such undesired configurations with additional penalty terms which were expensive to compute. After the minimization of the energy a postprocessing step was needed, because the connections are modelled implicitly by incidence relations. In fact, this postprocessing step is a local fibre tracker working on the line segments itself. Our approach is different: We avoid the postprocessing step, model the connections explicitly, and use common local fibre tracking as an optimization step. It is a graph-like model, where the line segments are the nodes and the fibres itself are connections between the nodes. In this way it is easy to fulfill the condition that one endpoint of a segment can only be connected to one other segment. So, problems like Y-junctions can not occur. Another difference is that not-connected segments feel just the external

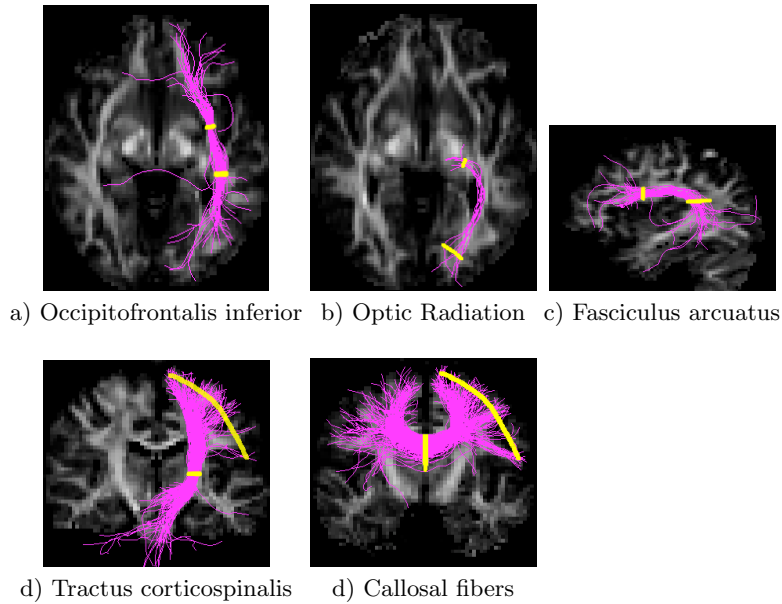


Fig. 3. The five considered selections. The fibre bundle projection are shown in magenta. The ROIs used for selection in yellow and the underlying image is an FA image.

energy. Only if a segment is connected it feels a certain regularization force making the fibre smooth and their curvature low. By the explicit modelling of the connections we introduced a huge combinatorial problem which seems difficult to solve. And indeed it is, if one had not the local methods that guide the search. We proposed to use a simple probabilistic fibre tracking algorithm for establishing the connections as a proposal distribution inside the Metropolis-Hastings algorithm. This idea makes the optimization feasible and efficient.

For a preliminary evaluation of our approach we used the same in vivo diffusion measurements as in [8]. The whole brain was covered with contiguous 2 mm slices in an in-plane resolution of $2 \times 2\text{ mm}^2$. The diffusion encoding was performed in 61 directions with an effective b-value of 1000 s/mm^2 . Additionally, a T_1 data set was acquired which was segmented into WM, GM, and CSF using SPM5 (<http://www.fil.ion.ucl.ac.uk/spm>). In comparison to Kreher et al [8] we only need the WM-mask to restrict the domain of reconstruction. In Kreher's approach also a preprocessing step is needed involving WM and GM to create a priori docking slots for the fibres. For the selection of specific fibre bundles we use the same ROIs as in [8] based on the WFU PickAtlas. In Figure 3 the ROIs are depicted in yellow. Our algorithm includes several parameters which have to be set. For the external energy there is: σ the spatial 'width' of a segment, c the orientational 'width' of a segment and w the weight of a segment. We adapted c to values found in voxels within the corpus callosum, that

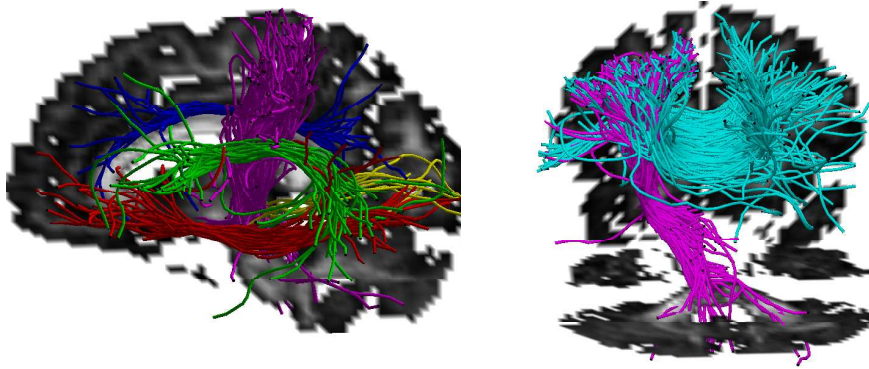


Fig. 4. The Occipitofrontalis inferior (red), the optic radiation (yellow), the Fasciculus arcuatus (green), the Tractus corticospinalis (magenta) and the callosal fibres (cyan).

is $c = 1$. Thus, each segment contributes with an apparent diffusion coefficient of $D = c/b = 10^{-3} \text{ mm}^2/\text{s}$. Both, w and σ influence the expected fibre density. They have to be tuned such that the computation time stays reasonable while the fibre density is as high as possible, we have chosen $w = 0.2$ and $\sigma = 0.4 \text{ mm}$. The internal energy has basically two parameters: the segment length was chosen to be $\ell = 1.6 \text{ mm}$ and the connection likeliness $L = 0.5$, while ℓ is controlling the smoothness and accuracy of the reconstruction and L the length of the fibres. Finally there are λ_{int} , λ_{ext} and the temperature T which express the relative weightings of the energies and the sharpness of the distribution. Due to the occurring ratios we can, without restrictions, set $\lambda_{\text{ext}} = 1/C$. Relative to that we set $\lambda_{\text{ext}} = 0.065$ and we started the algorithm with $T = 0.1$ and finished with $T = 0.001$ during $5 \cdot 10^8$ iterations (compare to [8] where $5 \cdot 10^9$ iterations were used). Using the above setting the optimization takes on standard PCs depending on the speed of the system between 12 and 24 hours. The results are concluded in Figure 3 and Figure 4. We obtained a system with about 2.5 million fibre segments arranged in approx. 80000 fibres. Compare this to the number of white matter voxels of about 70000. This means on average we have about 35 fibre segments passing one voxel. Remember that a fibre has a length of $2\ell = 1.6$ voxelunits, so one can claim that on average 35 fibres are crossing each voxel. In Figure 3 we used the ROIs to select five different fibre bundles. The bundles are shown as projections in magenta. Our algorithm is even able to detect the optic radiation fibres (shown in 3b)) which is a difficult task because they are in the vicinity of the dominant inferior longitudinal fasciculus and the corpus callosum. In Figure 4 we show the fibre bundles in 3D. For a visual comparison with the Gibbs-Tracker [8] and two other approaches (FACT [3] and PiCo [6]) see [8].

5 Conclusion

A novel global fibre reconstruction approach was proposed. The approach has broken down the computation times from one month, which recent global tracking algorithms needed, to below one day while keeping the performance. The key idea is to use common local tracking algorithm as optimization steps in a global framework. For future work validation is a key issue which includes extensive examinations of the dependencies on the parameters which occur inside the algorithm.

Acknowledgements

The work of M. Reisert was supported by European Commission, contract 027294 (I-KNOW). Further acknowledgements go to Susanne Schnell and Björn Kreher for various help and providing the ROIs.

References

1. Moseley ME, Cohen Y, Kucharczyk J, Mintorovitch J, Asgari HS, Wendland MF, Tsuruda J, Norman D. Diffusion-weighted mr imaging of anisotropic water diffusion in cat central nervous system. *Radiology* 1990;176(2):439–45. 0033-8419 Journal Article.
2. Conturo TE, Lori NF, Cull TS, Akbudak E, Snyder AZ, Shimony JS, McKinstry RC, Burton H, Raichle ME. Tracking neuronal fiber pathways in the living human brain. *Proc Natl Acad Sci U S A* 1999;96(18):10422–7. 0027-8424 (Print) Journal Article Research Support, Non-U.S. Gov't Research Support, U.S. Gov't, P.H.S.
3. Mori S, Crain BJ, Chacko VP, van Zijl PC. Three-dimensional tracking of axonal projections in the brain by magnetic resonance imaging. *Ann Neurol* 1999; 45(2):265–9. 99142739 0364-5134 Journal Article.
4. Basser PJ, Pajevic S, Pierpaoli C, Duda J, Aldroubi A. In vivo fiber tractography using DT-MRI data. *Magn Reson Med* 2000;44(4):625–32. 20481737 0740-3194 Journal Article.
5. Hagmann P, Thiran JP, Jonasson L, Vandergheynst P, Clarke S, Maeder P, Meuli R. Dti mapping of human brain connectivity: statistical fibre tracking and virtual dissection. *Neuroimage* 2003;19(3):545–554. English 1053-8119.
6. Parker GJM, Haroon HA, Wheeler-Kingshott CAM. A framework for a streamline-based probabilistic index of connectivity (pico) using a structural interpretation of mri diffusion measurements. *J Magn Reson Imaging* 2003;18(2):242–254. English 1053-1807.
7. Mangin J. A framework based on spin glass models for the inference of anatomical connectivity from diffusion-weighted mr data - a technical review. *NMR Biomed* 2002;15(7-8):481–492.
8. Kreher BW, Mader I, Kiselev VG. Gibbs tracking: a novel approach for the reconstruction of neuronal pathways. *Magn Reson Med* 2008 Oct;60(4):953–963.
9. Stoica R, Descombes X, Zerubia J. A gibbs point process for road extraction from remotely sensed images. *Int J Comput Vision* 2004;57(2):121–136. English 0920-5691.
10. van Lieshout MNM. *Markov Point Processes and Their Applications*. London: Imperial College Press, 2000.